Available online at www.sciencedirect.com
SCIENCE DIRECT
Tectonophysics 420 (2006) 333–343
TECTONOPHYSICS
www.elsevier.com/locate/tecto

Modeling sideswipe in 2D oceanic seismic surveys from sonar data: Application to the Mariana arc

Roland H. Günther [a,*], Simon L. Klemperer [a], Andrew M. Goodliffe [b]

[a] Department of Geophysics, Stanford University, CA 94305-2215, United States
[b] Department of Geological Sciences, University of Alabama, Box 870338, Tuscaloosa, AL 35487, United States

Received 27 January 2005; received in revised form 2 November 2005; accepted 6 January 2006
Available online 2 May 2006

Abstract

In two-dimensional (2D) marine seismic-reflection surveys, out-of-plane rough seafloor bathymetry can cause multiple ocean-bottom reflections that complicate the interpretation of shallow reflections. Although migration corrects for the in-plane position of reflectors, it cannot resolve the inherent ambiguity in their out-of-plane positions. We show how swath bathymetry, routinely collected in many such surveys, can be used to model out-of-plane seafloor reflections and prevent their misinterpretation as subsurface geology. We use both raw and gridded multi-beam bathymetry data to build images that represent seafloor reflections in migrated seismic data. Comparison of these images to the seismic sections reveals whether suspicious features are out-of-plane water bottom reflections or subsurface reflections. Multi-channel seismic surveys across the Marianas intra-oceanic arc system provide examples where rough seafloor topography produced reflections that were initially misinterpreted. We use our seafloor reflection modeling (SRM) approach to help distinguish a possible landslide from a volcanic cone, to help distinguish real from apparent fault-plane reflections bounding a sediment-filled basin, and to verify that a possible magma chamber reflection results from sub-surface structure, not seafloor sideswipe.

Keywords: Sideswipe; Sonar; Seismic reflection; Mariana arc

1. Introduction

Crustal-scale multi-channel seismic (MCS) reflection surveys routinely image deep structure on regional transects (e.g. Klemperer and Hobbs, 1991), but logistic and financial constraints almost always limit these surveys to 2D acquisition geometries. Whereas migration can properly represent the in-plane position of reflectors in 2D MCS data, it cannot properly place out-of-plane reflectors. For many large-scale crustal features, the dips of major reflectors are sufficiently flat that wave paths are essentially vertical, and where feasible surveys are designed as dip-lines (e.g. Yilmaz, 2001). However, complicated or unpredictable geometries often undermine these assumptions, especially for near-surface features. The result is a confusing image of the subsurface that does not accurately reflect a cross-section of the geology. The interpretational pitfalls resulting from out-of-plane seismic energy on 2D

* Corresponding author. Current address: Halliburton Digital and Consulting Solutions, 1805 Shea Center Drive, Suite 400, Highlands Ranch, CO 80129, United States. Tel.: +1 650 450 0266; fax: +1 303 796 0807.
E-mail addresses: rgunther@stanfordalumni.org (R.H. Günther), sklemp@stanford.edu (S.L. Klemperer), amg@ua.edu (A.M. Goodliffe).

0040-1951/$ - see front matter © 2006 Elsevier B.V. All rights reserved.
doi:10.1016/j.tecto.2006.01.027

profiles remain the subject of ongoing research (e.g. Drummond et al., 2004).

The impedance contrast at the seafloor is often large, so rough topography can produce out-of-plane seafloor diffractions or reflections (sideswipe) with large amplitudes (e.g. Larner et al., 1983; Newman, 1984). Depending on the location of the scatterer or reflector, seafloor reflections will appear on common-midpoint (CMP) gathers with apparent move-out velocities ranging from the water velocity for reflectors 90° from the profile heading to infinite velocity (constant arrival time) for point scatterers or reflectors directly ahead or astern along the profile. Thus reflections and diffractions returning from specific azimuths will tend to be enhanced on the CMP stack at specific two-way traveltimes depending on the stacking-velocity function in use (Newman, 1984). Similarly, reflected refractions (refracted or turning waves reflected from shallow discontinuities such as fault offsets) will show move-out in CMP gathers, appear as backscattered coherent noise, and may be enhanced during stacking (Day and Edwards, 1983; Calvert, 1997).

While subsurface out-of-plane reflections are a problem for all 2D surveys, seafloor sideswipe primarily affects deepwater surveys. Profiles acquired in shallow water are typically processed with a stacking velocity that increases rapidly with depth, arising from an interval velocity that increases rapidly with depth, thereby successfully mitigating all but the strongest sideswipe that has a move-out corresponding to water velocity. In contrast, profiles collected in oceanic water depths do not allow easy distinction between side-scattered reflections from off-line bathymetric highs and reflections vertically beneath the seafloor at equally late travel-times, because both have similar stacking velocities due to the long travel-time path in the water column despite potentially large differences in their interval velocities. Additionally, because the areal airgun arrays in common use focus source energy downwards, prominent side reflections tend to be returned from reflectors less than ca. 45° from the vertical at the dominant frequency. In shallow water, such reflectors are reasonably close to the acquisition profile, whereas in oceanic water depths (ca. 4 to 5 km) energy radiated at only 20° to 30° away from the vertical will insonify ocean floor ca. 2 to 3 km from the axis of the seismic profile. Correspondingly, prominent side reflections (from 0 to 30° off-axis) follow a seafloor reflection from 100 m depth delayed by only 0 to 20 ms but follow the seafloor reflection from 5 km water depth by 0 to 1 s travel-time. Hence out-of-plane seafloor reflections are much more likely to be confused with sedimentary features or tectonic structure in deep-water surveys.

In this paper we use multi-beam-sonar bathymetry data to forward model off-axis seafloor reflections in both zero-offset and migrated sections. Seafloor reflection modeling (SRM) provides a convenient, automatable and robust tool for identifying seafloor sideswipe in MCS data, and resolving interpretational ambiguities. The method does not predict out-of-plane diffractions, which are not properly collapsed by 2D migration since they have a different shape than in-plane diffractions.

2. Method

Swath bathymetry collected concurrently with a seismic profile may be used to construct images that simulate both in-plane and out-of-plane seafloor reflections in the migrated seismic sections. Such images can be constructed either from processed bathymetry grids (three-dimensional seafloor reflection modeling, 3D SRM) or directly from unprocessed swath bathymetry data (2D SRM). In both cases, we calculate the seismic wave produced and recorded by a single coincident source–receiver pair, or the so-called zero-offset arrival that CMP stacking aims to emulate. We assume that the seafloor produces discrete, specular reflections that appear in the seismic profile wherever the seafloor is parallel to the incident seismic wave front.

2.1. 3D SRM

Starting with a bathymetry grid, we determine for each seismic source location the points on the seafloor that would reflect a seismic wave back to the source. For a surface source point at $x=0$, $y=0$, $z=0$, we find seafloor reflection points by calculating the travel-time function $t(x, y, z)$ for the seismic wave from the source to each bathymetric grid point within a certain radius. For our Marianas examples, we used radii of 10 km, corresponding to two-way reflection times up to ca. 13 s. At seafloor points where $t(x, y, z)$ is a local minimum or maximum, the seafloor is orthogonal to the incident seismic wave and reflects the wave back to the source (Fig. 1, left). We can create an image of seafloor reflections for direct comparison with the unmigrated seismic profile by plotting the seafloor reflections observed at each source-point. Alternatively, we can create an image of seafloor reflections for direct comparison with the migrated seismic profile by plotting the travel-time to seafloor reflectors from the closest point on the line.

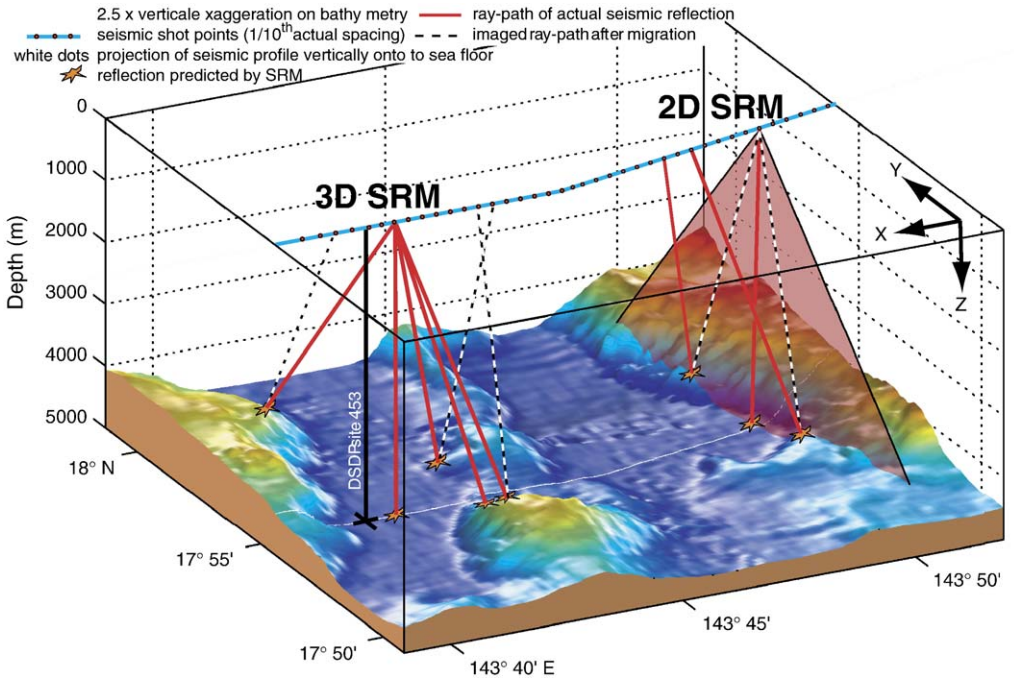

Fig. 1. Schematic of 3D and 2D SRM, drawn for the bathymetry at the site of DSDP hole 453 (see Fig. 4D) shown with ca. 2.5× vertical exaggeration. In 3D SRM, travel-times are calculated for an area surrounding each shot-point and unmigrated seismic reflections (red ray-paths) are identified wherever the travel-time function is a local minimum or maximum. The travel-times from reflection points to the closest shot points are calculated to model the image of the reflectors in a migrated seismic section (dotted ray-paths). In 2D SRM, ray-paths represented by the migrated seismic section (dotted ray-paths) are already located in the plane of the sonar fan. However, the actual ray-paths of reflected seismic waves (red ray-paths) may occur in a different plane. Note that differences between real and image ray-paths are exaggerated.

For this zero-offset model, the nominal horizontal resolution is the spacing of the source points. Since the horizontal resolution of migrated MCS profiles, the CMP spacing, is typically smaller than the source spacing, it is necessary to interpolate additional source points in order to achieve the same theoretical resolution. This is particularly important in one of the data sets we show subsequently (Example 1 in Fig. 2), acquired principally as a crustal refraction survey but recorded simultaneously on an MCS streamer, for which source-points occur only every 20th CMP.

Because our 3D SRM method relies on gridded bathymetry, any available data set of sufficiently high resolution may be used, as we demonstrate for Example 1 (Figs. 2 and 3). Correct geographic registration of data sets of different vintages, acquired with different navigation systems, may present a problem. 3D SRM may also be used to predict the impact of sideswipe during the design phase of a survey.

2.2. 2D SRM

We can also construct an image of migrated seafloor reflections directly from swath sonar data that has not been mapped to a bathymetry grid, so long as the seismic and sonar data are collected concurrently. For each sonar ping, a multi-beam sonar system uses collimated beams to collect travel-times along a fan that is orthogonal to the ship heading, which is nominally identical to the azimuth of the seismic profile (Fig. 1, right). Note that the seafloor is not necessarily orthogonal to the sonar beam at these points: the use of high-frequency beam-forming sources allows multi-beam systems to measure travel-times from non-orthogonal back-scatter. At points along each fan where the travel-time is a local minimum or maximum, the seafloor is orthogonal to the sonar wave with respect to the cross-track dimensions. These seafloor points may not produce reflections for the equivalent seismic source–receiver pair (at the same position as the sonar source) because the low-frequency seismic profile is dominated by reflections off surfaces orthogonal to ray-paths in both dimensions. But a seafloor point that is orthogonal to the seismic wave in the cross-track dimension will be orthogonal in both dimensions for some source–receiver pair along the reflection profile and will produce a reflection in the stack at the corresponding location. Since 2D migration moves the

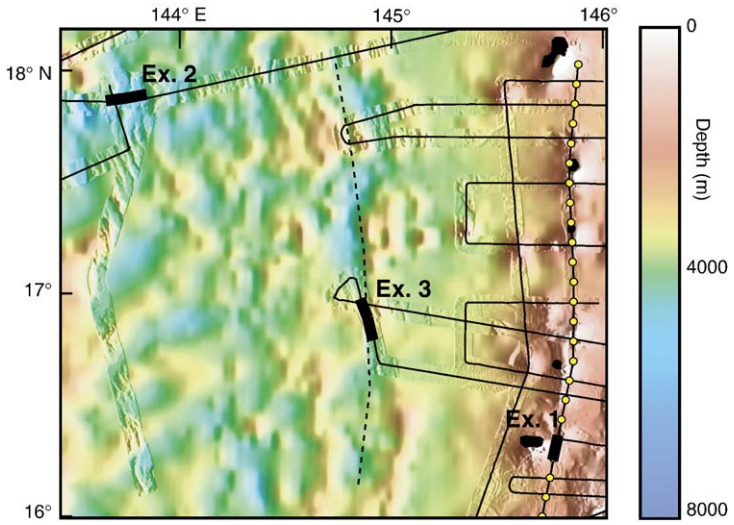

Fig. 2. Bathymetry map of the Marianas arc and back-arc; dashed line marks approximate location of the spreading center and black blobs along eastern edge of the map are island volcanoes. Thin black lines are MCS profiles and yellow circles mark ocean-bottom seismometer locations for an associated crustal refraction profile. SRM examples (heavy black lines) are shown at a possible slide-block on the south-east slope of the volcano Anatahan (Example 1, shown in Fig. 3), a basin at the western edge of the extensional trough (Example 2, shown in Fig. 4), and a suspected magma chamber (Example 3, shown in Fig. 5).

energy of these reflections back to the closest CMP, the imaged ray-path is the same ray-path observed by the sonar system. To build a synthetic image of seafloor reflections in migrated seismic data, we use the sonar travel-time minima and maxima detected at each sonar source point as a proxy for seismic reflections imaged at each CMP. This method depends on the orientation of the sonar system relative to the seismic profile and thus requires bathymetry data collected concurrently with the seismic profile.

3. Applications

The *R/V Maurice Ewing* was used to acquire regional crustal seismic surveys of the Marianas fore-arc, arc, and back-arc regions in 2002 (see Stern et al., 2003, for a review of the tectonic setting). Cruise EW0202 acquired conventional deep-crustal MCS profiles using a single 6 km streamer with 25 m group spacing to record a large, tuned airgun array fired at 50-m intervals (Taylor et al., 2002). Cruise EW0203 used a similar airgun array fired at intervals of 200 m to 250 m to acquire crustal wide-angle data, but also recorded these sparse shots with the same 6 km streamer (Kerr et al., 2002). In several regions, and on both surveys, rough seafloor topography produced sideswipe that interfered with the interpretation of reflections within about a second of the water-bottom. Our data-processing utilized a standard sequence: Read in SEG-D data; Load Geometry into headers; Shot mute to remove water column noise; Trace edit based on trace statistics; 4–6–60–70 Hz Ormsby filter; Construct supergathers; Velocity analysis; Pick top and bottom mutes; Apply NMO; Apply mutes; Stack; Construct migration velocity model; Stolt migration; Pick seafloor mute.

We used both 2D and 3D SRM to investigate the effects of seafloor topography on our reflection sections. The 2D SRM is based on unprocessed travel-time measurements by a 140-beam Krupp Atlas Hydrosweep DS2 multi-beam sonar system. For the 3D SRM we used two bathymetry data sets, one gridded at 150 m which was collected simultaneously with our seismic data, and one gridded at 50 m which was collected on a subsequent cruise that overlapped in part with our reflection profiles (Embley et al., 2004; Chadwick et al., 2005). We produced SRM models for the entire ca. 8000 km of seismic profiles but only present results here for three specific examples of geologic interest (Fig. 2).

3.1. Example 1: Volcanic cone initially interpreted as submarine landslide

Anatahan, one of the largest active volcanoes in the Mariana arc, began its first historical eruption cycle in 2003 (Hilton et al., 2005). Outstanding scientific questions about volcanoes such as Anatahan concern the total volume of eruptive products and the means by which these products are distributed away from the

volcano, both during the eruptive phase and subsequently by mass-wasting. Lateral flank-collapse deposits are recognized adjacent to island volcanoes in nearly every ocean (Moore et al., 1994) and are believed to represent a tsunamogenic hazard (Keating and McGuire, 2000). It was therefore of potential geologic interest when an apparent topographic prominence was noted on our 2D-migrated seismic profile, on the flank of Anatahan ca. 8 km from the summit, rising ≥400 ms above the seafloor (Fig. 3A). The continuity of a reflection following the first arrival could be consistent either with a slide plane beneath a large submarine landslide (cf. Dingle, 1983) or with a vertical seafloor reflection beneath an out-of-plane seafloor reflection back-scattered from a satellite volcanic cone. The absence of an upward bend underneath the protrusion is a preliminary indication that the continuous reflection is sideswipe. The velocity of a slide block would be larger than the velocity of the surrounding water and would cause "velocity pull-up" on an underlying reflection in our time migrations. This profile was collected during airgun shooting for refraction recording, and so has source points only every 200 m and is a 15-fold data set with CMPs every 12.5 m.

We were able to carry out SRM using both a 3D high-resolution data set collected on a subsequent cruise (Chadwick et al., 2005), and the 2D swath mapping collected simultaneously with our own reflection profiles. The 3D SRM shows both the protruding first-arrival and the top and bottom segments of the continuous MCS reflection (Fig. 3B), suggesting that the continuous reflector results from the seafloor but that the bathymetry grid lacks the resolution to model the entire length of the reflection (note that the lower blue line is not continuous). The 2D SRM, based on the denser multi-beam data, shows that the entire length of the continuous reflection results from the seafloor (Fig. 3C). SRM provides a very clear result that the MCS profile images two seafloor reflectors, separated by 400 ms, and that the correct interpretation is of sideswipe from an offline topographic prominence, not of an inline slide block. Mapping the reflection points directly onto the topographic map (Fig. 3D) shows the twin lines of

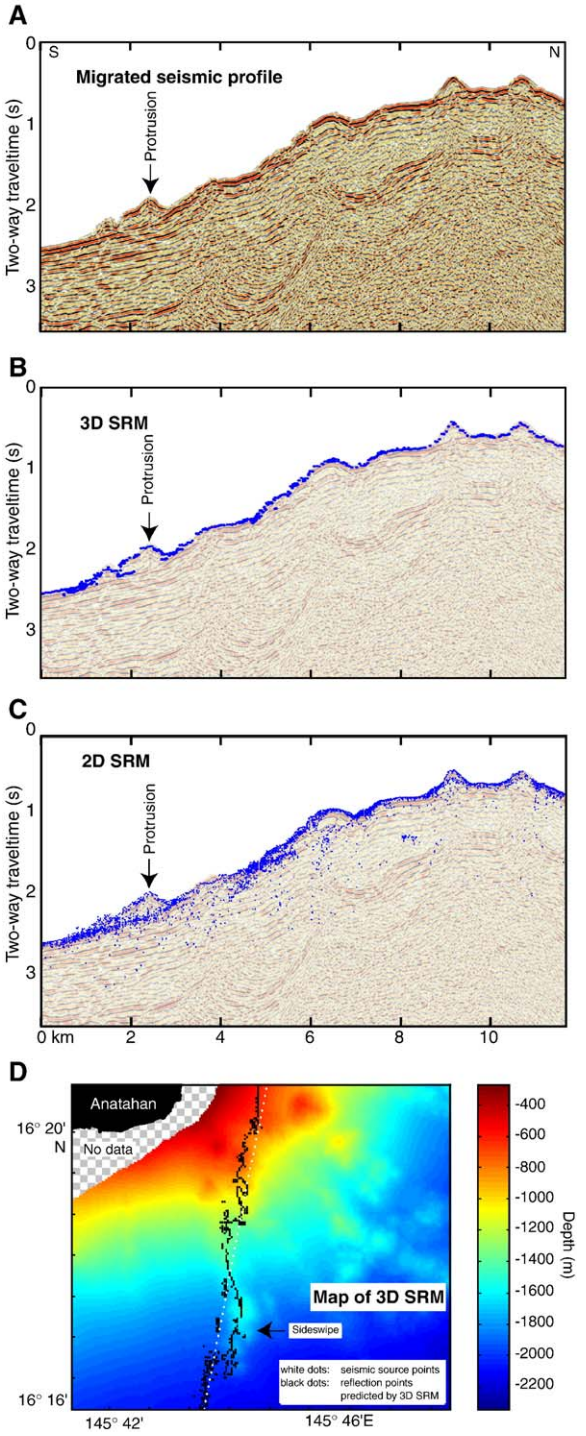

Fig. 3. (A) Seismic section of the southeastern slope of Anatahan (ca. 2× vertical exaggeration at the seafloor); note the protruding reflection (preliminarily interpreted as a slide block) preceding an otherwise continuous seafloor reflection by up to 400 ms. (B) 3D SRM predictions (blue dots) suggest both the protruding reflection and at least part of the continuous reflection originate at the seafloor. (C) 2D SRM (blue dots) images the entire length of the continuous reflection. Although these 2D predictions achieve higher resolution and indicate additional sideswipe events (e.g. at km 4 to 6), they are less coherent than the 3D results. (D) Mapping of 3D SRM reflection points onto bathymetry shows the continuous reflection results from the seafloor reflection directly beneath the profile whereas the protrusion results from reflections from an off-line topographic feature ~1 km east, probably a group of constructional volcanic cones (Chadwick et al., 2005).

reflection points at the seafloor arising from the single line of airgun sources, and makes it clear that the first arrival is indeed sideswipe. Although our seismic data cannot show whether the offline topography is a volcanic cone or a slide block, because the potential discriminant (the "slide plane" beneath the block) is simply an artifact of 2D data acquisition in a 3D world, recent geologic mapping based on backscatter data coupled with the bathymetry shows the feature as a group of eruptive vents (Chadwick et al., 2005).

The difference in character between the 2D and 3D models (Fig. 3B and C) is largely the result of processing, especially smoothing, that has been applied to the bathymetry grid used for 3D SRM, but not to the raw data used for 2D SRM. Some of the predicted reflection points in the 2D model are likely the result of noise in sonar travel-time measurements, though here there is no evidence of coherent noise such as we address subsequently (Example 3 below). Whereas the 3D model provides a cleaner image of the sideswipe, it predicts only part of the continuous reflector and thus in other areas may fail to identify sideswipe events. Since we prefer to err on the side of over-predicting sideswipe and under-interpreting geology, 2D SRM is the main focus of subsequent examples.

3.2. Example 2: Basins in the back-arc basin: normal faults or onlap against volcanic edifices?

One of our profiles with very prominent off-axis reflections transects a deep and narrow sediment-filled basin on the western edge of the Mariana back-arc basin (for bathymetry see Fig. 1; for 2D-migrated seismic data see Fig. 4A). Deep Sea Drilling Site (DSDP) site 453, located on the western edge of the basin, recovered 455.5 m of clastic sediments above 149.5 m of coarse breccias (Hussong et al., 1982). These breccias may represent a landslide deposit formed within the basin (Natland, 1982). Two predominantly east–west MCS profiles were collected at the time of drilling, but their locations 5 km north and south of the site (Fig. 4D) prevent reliable correlation between the core and the reflection profile. Sideswipe further complicates the correlation by obscuring the basin stratigraphy (Mrozowski et al., 1982).

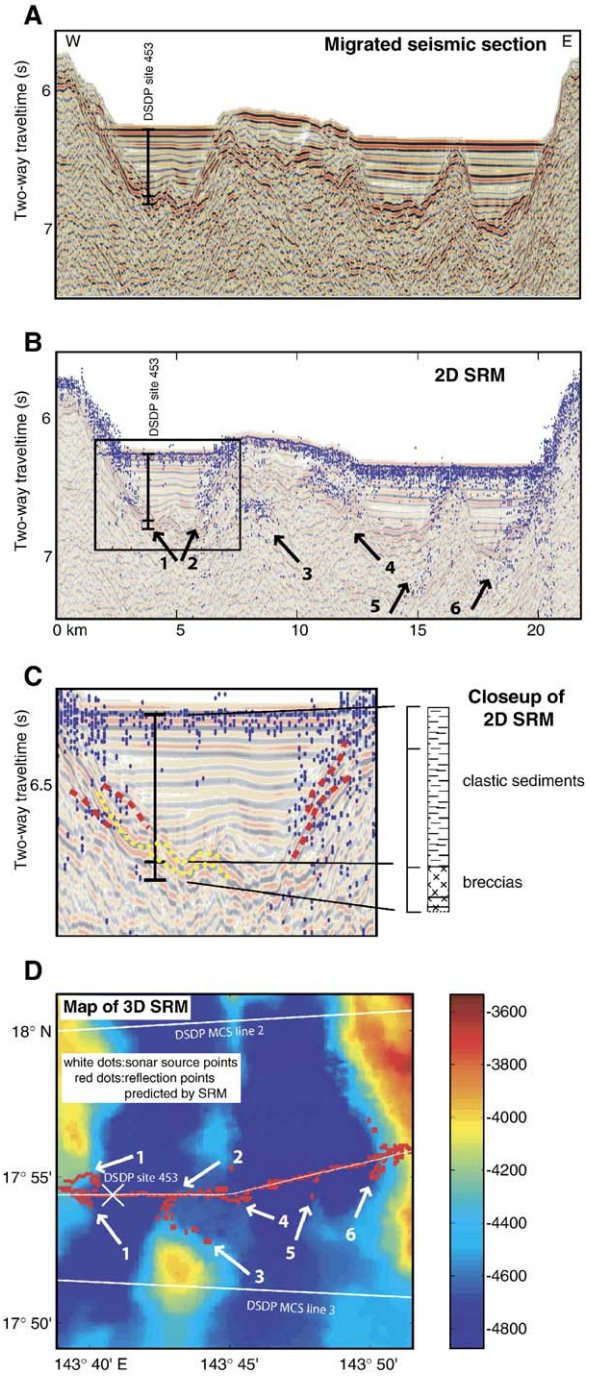

Fig. 4. (A) Seismic profile in the back-arc basin (ca. 7× vertical exaggeration at the seafloor) seems to show clearly defined boundaries (faults?) between basement rock and sedimentary fill. (B) 2D SRM indicates that sideswipe contaminates the seismic image of the basin walls. Arrows 1–6 indicate sideswipes identified in map view in (D). (C) Enlargement of profile and 2D SRM over DSDP site 453 shows two steeply dipping phases, marked with red dashed lines and interpreted as sideswipe, and two less steep reflections, marked with yellow dotted lines and interpreted as real subsurface structure. All four arrivals are close to the transition from sediments to breccias at 455 m. (D) Mapping of the reflection points onto the bathymetry map shows that the seafloor reflections track along the basin walls. Numbers correspond to sideswipes highlighted in B.

Our east–west MCS profile (Fig. 4A), crossing directly over the drill site, provides a clearer image than the previous 20-year-old profiles (not shown). Although 2D migration collapses many of the seafloor diffractions in the stack, the section still shows intersecting reflections at the basin walls, particularly at the western margin of both basins. Our preliminary interpretation was that these intersecting reflections represent subsurface faces of the basin walls (perhaps normal faults, because they continue >1.5 s below the seafloor) reflected from out-of-plane (sideswipe reflected refractions, because they intersect with sedimentary reflections even after 2D migration). Reflected refractions or turning-wave reflections from heterogeneities at or near the seafloor (cf. Calvert, 1997, his Fig. 1) appear on a stack section as nearly linear coherent arrivals with apparent dips related to the angles between the features and the seismic line. After migration these arrivals can extend close to the direct image of the feature that produced them, leading to the possibility that they may be misinterpreted as faults (Calvert, 1997).

A significant geologic uncertainty is whether the basins imaged by our MCS data represent passive sedimentary infilling of volcanic topography, or genuine rifts with bounding normal faults. At DSDP site 453, stratal thickening westward towards the basin margin, from 6.5 to 6.8 s two-way time, suggests an east-dipping normal fault; however equally sharp reflection truncations on the eastern and western margins of both basins (Fig. 4A) support interpretation as full-grabens as opposed to half-grabens or purely volcanic topography. Our profile was collected purely as a reflection profile, with source points every 50 m. Our 2D-SRM model (Fig. 4B and C) and our 3D-SRM model (not shown) indicate that many of the seemingly subsurface reflections actually result from exposed basin walls, particularly reflection trends 2, 5 and 6 on the eastern margins of the basins. Mapping these sideswipe reflection points onto the seafloor (Fig. 4D) shows that reflections track the basin walls for considerable distances (1 to 2 km) from the source profile. The recognition, via SRM, that dipping reflection trends #2, 5 and 6 (Fig. 4B and D) are possibly entirely of out-of-plane seafloor origin argues against the existence of fault-plane reflections on the eastern margins of these basins. If these basins are in part formed by extension, it is probably as half-grabens above east-dipping faults on their western margins along trends #1 and 4.

In the vicinity of the drill-hole, our 2D-SRM model helps to make sense of the conflicting reflections and possibly identifies a reflector that could mark the transition from clastic sediments to coarse breccias (Fig. 4C). The SRM model identifies a series of side-reflection travel-times that coincide with the top of a steeply dipping reflection (upper dashed line in Fig. 4C; trend #1 in Fig. 4B) that intersects with the sediment reflections. It seems likely that the entire seismic reflection originated at the seafloor though the sonar resolution is sufficient only to image part of its length. Beneath this reflection, our SRM model predicts a second, shorter reflection with a similar dip (lower dashed line in Fig. 4C). Two strong, lower-frequency reflections with varying dip (dotted lines) seem to originate from real subsurface structure and may correspond to the slide interpreted by Natland (1982). These reflections extend across the basin with the hummocky shape that is characteristic of slides and their depth is approximately consistent (within about a wavelength) with the travel-time expected from core velocity measurements (from Hussong et al., 1982), although in a region with steeply dipping structure oblique to the profile true depths to reflectors are impossible to determine without a 3D survey. We note that the resolution of our 2D model is sufficient to make a tentative interpretation here but is generally too coarse to allow for the interpretation of individual reflections. Higher-resolution sonar data could decrease the scatter for the SRM predictions and make such detailed interpretations possible.

The interpretational uncertainty in this environment is the potential origin of dipping reflections either from dipping fault-planes, or from unfaulted, surface or subsurface dipping sediment–basement interfaces, on the flanks of a basin in which there is little lateral stratal thickening to determine fault polarity. This uncertainty is well demonstrated in conflicting published interpretations of the west–east continental-margin seismic profile CM-16 of Montadert et al. (1979) across the Goban Spur, Bay of Biscay. This profile, influential on ideas about passive-margin formation, was initially interpreted as showing half-grabens bounded by oceanward-dipping listric faults (Montadert et al. (1979), and subsequently re-interpreted based on 2D travel-time modeling as imaging dominantly landward-dipping faults (Peddy et al., 1986). More widespread data acquisition across the region has reaffirmed the initial oceanward-dipping interpretation (Le Pichon and Barbier, 1987; Thinon et al., 2003). Published fault-trend maps (Montadert et al., 1979) and bathymetric analyses (Lallemand and Sibuet, 1986) show sub-surface and surface NNW trends that cut obliquely across the disputed west–east seismic profile suggesting that the 2D profile recorded out-of-plane energy from both surface and subsurface features that complicated the

interpretation of fault-planes, just as in our example from the Mariana back-arc basin (Fig. 4).

3.3. Example 3: Magma chamber reflection originally interpreted as sideswipe

Taylor et al. (2002) reported a reflection in the back-arc spreading center that might result either from a magma chamber or side-scatter from a nearby topographic ridge (Fig. 5A). Magma chamber reflections have been interpreted beneath several oceanic spreading centers including the Juan de Fuca Ridge (e.g. Morton et al., 1987, from 2D reflection profiles) and the East Pacific Rise (e.g. Kent et al., 2000, from a 3D survey); these seismic images of melting beneath ocean ridges provide important clues about the formation of oceanic crust. However, the rough topography of the ridges makes misinterpretation of sideswipe a likely pitfall, as acknowledged in some prior studies (e.g. Petersen, 2000). In our example, sonar artifacts created some complications, but SRM provides strong evidence that the relevant reflection represents real subsurface structure.

Fig. 5A shows the migrated reflection section recorded directly along the axis of the back-arc spreading center (Fig. 2). Beneath the flattest, shallowest part of the axis, a bright sub-horizontal reflection appears ca. 1.5 s after the seafloor reflection and may represent a magma-chamber reflection (Taylor et al., 2002). A steeper south-dipping reflection south of the putative magma-chamber reflection should not be a diffraction because this is a migrated section. The first seafloor multiple was tail-muted from the stack section before migration, so the south-dipping reflection cannot be the migrated multiple of the dipping seafloor vertically above it (and of course the migrated multiple of a dipping reflection is displaced laterally from the migrated primary).

Although the 3D SRM model (not shown) does not contain any indications of late-arriving seafloor reflections, the raw, unfiltered 2D SRM model (Fig. 5B) shows significant reflected energy up to 3 s after the first seafloor arrival. Note that this energy mimics the shape of the first arrival but does not closely match the

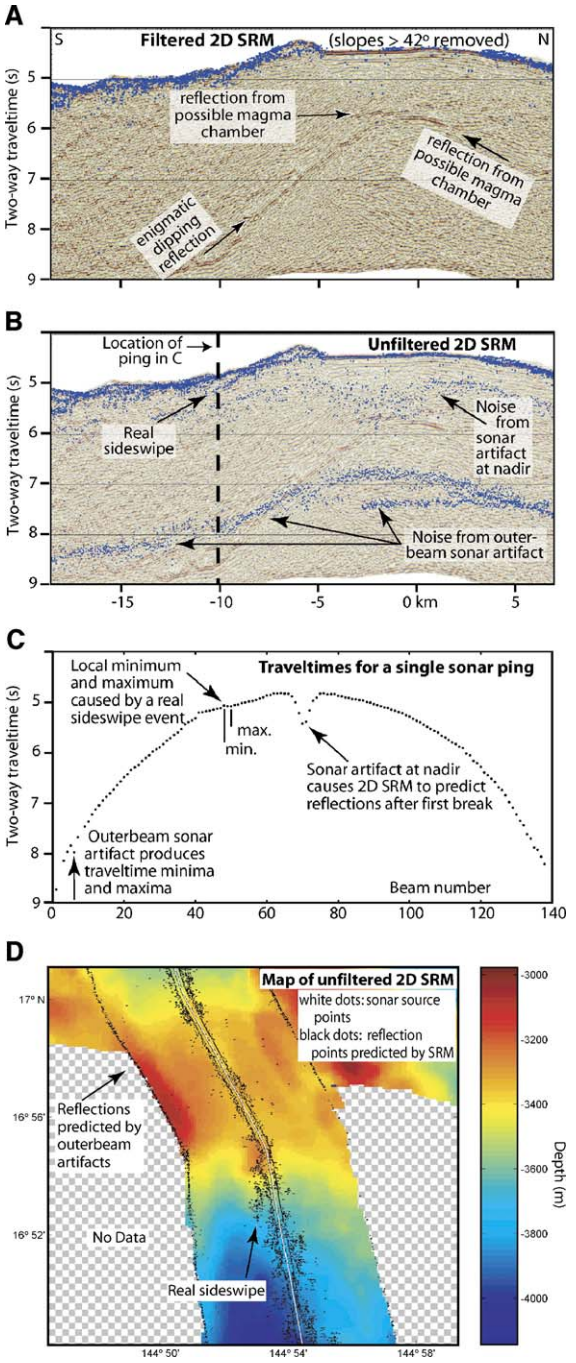

Fig. 5. Seismic profile across a possible magma chamber within the back-arc spreading center (ca. 3.5× vertical exaggeration at the seafloor), overlain by filtered 2D SRM predictions – filtering consists of removal of all sideswipes predicted from slopes that are >42° in the multi-beam data set, i.e. too steep to represent plausible seafloor topography. Note that all remaining predicted sideswipe arrives within 500 ms of the main seafloor reflection. (B) Same seismic section overlain by unfiltered (raw) 2D SRM shows strong signal several seconds after the first arrival that we interpret as artifacts of the multi-beam system. (C) Travel-times for a single sonar ping show typical multi-beam artifacts at the nadir and at the edge of the swath. (D) Mapping of the reflection points predicted by 2D SRM onto the bathymetry shows predicted reflections closely paralleling the center beam (the track of the sonar source points) and along the outer edges of the swath. Bathymetry data beyond the outer beam artifacts in the northern part of the region shown are provided by a crossing reflection profile (see Fig. 2).

suspected magma-chamber reflection. Analysis of a typical sonar ping (Fig. 5C) reveals that these reflections result from abrupt travel-time changes both at center and the edge of the swath. The map view (Fig. 5D) shows numerous modeled reflections originating at the outer edge of the swath coverage and along bands centered on the nadir. A Hydrosweep software upgrade that had not been calibrated at the time of our cruise may have contributed to this problem, but since such artifacts are common in multi-beam data, sonar data is often manually edited and/or filtered to remove unreasonably large slopes (Caress and Chayes, 1996). We use a similar slope filter to produce our filtered 2D model (Fig. 5A) that still shows a sideswipe event near the first arrival but does not predict sideswipe more than ca. 300 ms after the first arrival. Only a large topographic feature, well within the resolution of both models, could produce the reflection under consideration, which occurs more than 1 s beneath the seafloor and spans ca. 5 km. Both the 3D and filtered 2D models provide strong evidence that the putative magma-chamber reflection is indeed the result of subsurface structure. The dipping reflection remains enigmatic. The bathymetry map (Fig. 5D) shows inward-facing fault scarps bounding the axial valley. A "backwards projection" (not shown) of possible reflection points onto the bathymetry indicates that the valley walls are positioned to produce at least part of the reflection, yet SRM shows that their slopes are too gentle to produce a specular reflection in the right location. Obviously, the unknown topography too distant from the track-line to be mapped by the swath bathymetry (Fig. 5D) can only cause sideswipe reflections at travel-times later than the outer beam artifacts, and so cannot be the cause of the dipping reflection. A potential failing of SRM is its inability to model sideswipe back-scattered from features smaller than the resolution of our bathymetry model, here ca. 80 m laterally, but it seems implausible that a line of scatterers on the fault plane would individually be too small to register in the bathymetry model yet would line up so coherently over almost 10 km laterally. More likely the dipping reflection represents subsurface structure, possibly from out-of-the-plane (cf. Calvert, 1997), hence inappropriately migrated on this 2D section. This is a class of problem that our SRM models cannot address, and which requires multiple 2D profiles, or ideally 3D data, for proper analysis.

4. Discussion

Several processing steps can be used to remove noisy data and correct for ship orientation in standard work flows for converting raw multi-beam data into interpretable bathymetry grids. Since these steps have not been applied to the raw data used by the 2D model, sonar noise has the potential to degrade the accuracy of the model. Our basic model also makes numerous simplifications about acquisition geometry and the physics of seismic waves. Here we discuss a few potential problems and possible improvements.

Because the water velocity profile can cause significant curvature in sonar ray-paths (see, e.g. Blackinton, 1991; Caress and Chayes, 1996), ray-tracing is a common processing step for producing bathymetry, including the grids used for our 3D model. To improve the accuracy of the travel-time calculations for 3D SRM, we used ray-tracing to find the curved paths from the source points to each depth point. Given the resolution of our data set, we did not find an improvement in model quality sufficient to justify the far-greater computation time required for the ray-path inversions. Even if this correction does turn out to be significant for very high-resolution 3D models, it is not needed for the 2D model, which is built from time-domain sonar data and so is directly comparable to time-migrated seismic data.

Since our 2D models assume that the sonar ping is collected along a vertical swath that is orthogonal to the profile, a different ship heading (due to tides or currents) and short-period variations in both ship heading (yaw) and pitch due to rough seas would cause 2D SRM to predict seafloor reflections at incorrect locations on the profile. The magnitude of these effects depends on local currents and sea conditions, but for our survey, the lateral errors due to misaligned pitch were typically ca. ±5 m and occasionally ±20 m. Over a flat seafloor, ship heading does not affect the position of the inferred SRM reflection points, which remain vertically beneath the ship. For the more interesting examples presented here (Figs. 3–5) the topographic side-reflections that interfere with the subsurface reflections originate 1 km and even 2 km away from the ship-track. For yaw of ±5° these side reflections would be misplaced ±90 m to even ±180 m along the reflection profile. Even at our most detailed scale of observation (Fig. 4C) the along-track scatter of the modeled SRM reflection points that we infer may represent a single dipping reflection is several hundred meters. Though in this study we did not need to correct for effects of ship heading, sonar systems typically record the navigational information that is needed to map 2D predictions to their correct positions. Note that in the case of 3D SRM all effects of heading and pitch should have already been removed so our 3D methodology is immune to such problems.

In principle, seafloor reflection models of sufficient resolution could be adaptively subtracted either from pre-stack or stacked data. As presented here, SRM assumes that the seafloor produces only specular reflections, which are likely to be the strongest and most coherent events. While this approach is useful for interpretation, it does not accurately predict reflection amplitudes which is a requirement for effective adaptive subtraction. Several enhancements could improve the modeling of the amplitudes. For 2D SRM, it may be possible to directly use the beam amplitudes which are recorded by many of the multi-beam systems in common use. This approach would retain the advantage of 2D SRM of operating on unprocessed sonar data, but the result could only be subtracted from migrated data. Furthermore, due to the limited horizontal resolution of the unprocessed data, it would only provide an unaliased prediction at low frequencies. A true-amplitude 3D model can be constructed by using Kirchhoff summation over so-called exploding reflectors located at bathymetry grid points. Like 3D SRM, this approach cannot model seafloor features smaller than the sonar resolution, but it is easily extended to operate on pre-stack data, and the bathymetric grid can be interpolated as necessary to prevent spatial aliasing. Ultimately, adaptive subtraction may be unnecessary or even undesirable. It would be necessary to distinguish between in-plane and out-of-plane seafloor energy, else the subtraction would remove the in-plane water-bottom reflection as well as undesirable sideswipe. Nonetheless, these enhancements may increase the useful of SRM for interpretation.

5. Conclusions

The SRM methodology presented here makes it possible to quickly and confidently identify whether seismic reflections originated on the seafloor, and the examples show that it can help in making geological interpretations. Its utility depends on the availability of high-quality swath bathymetry data. Although it is possible to construct the 3D model from gridded bathymetry collected independently, we obtained our best results with 2D SRM, which requires multi-beam bathymetry collected concurrently with the seismic profiling. The simplicity of the 2D algorithm also presents significant time savings – the biggest challenge is accessing the raw multi-beam data (we used MB System, a software package published by Caress and Chayes (1996)).

Though useful as an interpretation tool, seafloor modeling does not solve the problem of sideswipe. As presented here, it does not remove sideswipe reflections from the data. More importantly, it cannot resolve the ambiguity in cross-track positions of subsurface reflectors. Though rarely used at sea, "wide-line" or multi-streamer 2D surveys could allow beam-steering or array-processing to identify and filter out sideswipe or other cross-line noise (Duren and Morris, 1992). More generally, 3D surveys would provide far superior imaging for the geologic examples in this paper. Although a handful of academic 3D surveys have been acquired (e.g. Kent et al., 2000), their enormous cost means that 2D surveys will remain the norm for academic regional and crustal studies for decades to come. For these surveys, SRM provides a fast and robust method for reducing the impact of sideswipe artifacts on our interpretations.

Acknowledgements

This study was made possible by the dedication of the Captain and crew of the *R/V Maurice Ewing* and shipboard science parties EW-0202 and EW-0203. Funding was provided by the NSF MARGINS program, awards OCE-0001956 and OCE-0001798. Bob Embley and Bill Chadwick generously provided "Ring of Fire" bathymetry around Anatahan, and the helpful comments of Brian Taylor, Stewart Levin, Barrie Taylor and Andy Calvert, and a review by Richard Hobbs, all helped improve this paper.

References

Blackinton, J.G., 1991. Bathymetric resolution, precision and accuracy considerations for swath bathymetry mapping sonar systems. IEEE Proceedings 550–556.

Calvert, A.J., 1997. Backscattered coherent noise and seismic reflection imaging of the oceanic crust; an example from the rift valley of the Mid-Atlantic Ridge at 23°N. Journal of Geophysical Research, B, Solid Earth and Planets 102 (3), 5119–5133.

Caress, D.W., Chayes, D.N., 1996. Improved processing of Hydrosweep DS multibeam data on the R/V Maurice Ewing. Marine Geophysical Researches 18 (6), 631–650.

Chadwick Jr., W.W., Embley, R.W., Johnson, P.D., Merle, S.G., Ristau, S., Bobbitt, A., 2005. The submarine flanks of Anatahan volcano, Commonwealth of the Northern Mariana Islands. Journal of Volcanology and Geothermal Research 146, 8–25.

Day, G.A., Edwards, J.W.F., 1983. Reflected refracted events on seismic sections. First Break 1 (9), 14–17.

Dingle, R.V., 1983. Slump structures on the outer continental margin of southwestern Africa. In: Bally, A.W. (Ed.), Seismic Expression of Structural Styles, Am. Ass. Petrol. Geol. . Studies in Geology, vol. 15, pp. 1.2.1–24–1.2.1–30.

Drummond, B.J., Hobbs, R.W., Goleby, B.R., 2004. The effects of out-of-plane seismic energy on reflections in crustal-scale 2D seismic sections. Tectonophysics 388 (1–4), 213–224.

Duren, R.E., Morris, S.V., 1992. Sideswipe removal via null steering. Geophysics 57 (12), 1623–1632.

Embley, R.W., Baker, E.T., Chadwick Jr., W.W., Lupton, J.E., Resing, J.A., Massoth, G.J., Nakamura, K., 2004. Explorations of Mariana Arc Volcanoes Reveal New Hydrothermal Systems. Eos Trans. AGU 85 (4), 37–40.

Hilton, D.R., Pallister, J.S., Pua, R.M. (Eds.), 2005. The 2003 Eruption of Anatahan Volcano, Commonwealth of the Northern Mariana Islands. Journal of Volcanology and Geothermal Research, vol. 146 (1–3), pp. 1–256.

Hussong, D.M., Uyeda, S., et al., 1982. Site 453: west side of the Mariana Trough. In: Hussong, D.M., Uyeda, S., et al. (Eds.), Init. Repts. DSDP, vol. 60, pp. 101–167.

Keating, B.H., McGuire, W.J., 2000. Island edifice failures and associated tsunami hazards. Pure and Applied Geophysics 157 (6–8), 899–955.

Kent, G.M., Singh, S.C., Harding, A.J., Sinha, M.C., Orcutt, J.A., Barton, P.J., White, R.S., Bazin, S., Hobbs, R.W., Tong, C.H., Pye, J.W., 2000. Evidence from three-dimensional seismic reflectivity images for enhanced melt supply beneath mid-ocean-ridge discontinuities. Nature 406 (6796), 614–618.

Kerr, B.C., Klemperer, S.L., EW0203 Scientific Party, 2002. Wide-angle imaging of the Mariana subduction factory. EOS, Transactions - American Geophysical Union 83 (47), F1319 Fall Meet. Suppl..

Klemperer, S.L., Hobbs, R.W., 1991. The BIRPS Atlas; Deep Seismic Reflection Profiles Around the British Isles. Cambridge University Press. pp. 128+99 sections.

Lallemand, S., Sibuet, J.-C., 1986. Tectonic implications of canyon directions over the Northeast Atlantic continental margin. Tectonics 5 (7), 1125–1143.

Larner, K., Chambers, R., Yang, M., Lynn, W., Wai, W., 1983. Coherent noise in marine seismic data. Geophysics 48 (7), 854–886.

Le Pichon, X., Barbier, F., 1987. Passive margin formation by low-angle faulting within the upper crust; the northern Bay of Biscay margin. Tectonics 6 (2), 133–150.

Montadert, L., Roberts, D.G., De Charpal, O., Guennoc, P., 1979. Rifting and subsidence of the northern continental margin of the Bay of Biscay. In: Montadert, L., Roberts, D.G., et al. (Eds.), Initial Reports of the Deep Sea Drilling Project, vol. 48, pp. 1025–1060.

Moore, J.G., Normark, W.R., Holcomb, R.T., 1994. Giant Hawaiian landslides. Annual Review of Earth and Planetary Sciences 22, 119–144.

Morton, J.L., Sleep, N.H., Normark, W.R., Tompkins, D.H., 1987. Structure of the southern Juan de Fuca Ridge from seismic reflection records. Journal of Geophysical Research 92 (11), 11315–11326.

Mrozowski, C.L., Hayes, D.E., Taylor, B., 1982. Multichannel seismic reflection surveys of Leg 60 sites, Deep Sea Drilling Project. In: Hussong, D.M., Uyeda, S., et al. (Eds.), Initial Reports of the Deep Sea Drilling Project, vol. 60, pp. 57–69.

Natland, J.H., 1982. Petrography and mineral compositions of gabbros recovered in Deep Sea Drilling Project Hole 453 on the western side of the Mariana Trough. In: Hussong, D., Uyeda, M., et al. (Eds.), Initial Reports of the Deep Sea Drilling Project, vol. 60, pp. 579–599.

Newman, P., 1984. Seismic response to sea-floor diffractors. First Break 2 (2), 9–19.

Peddy, C., Brown, L.D., Klemperer, S.L., 1986. Interpreting the deep structure of rifts with synthetic seismic sections. In: Barazangi, M., Brown, L.D. (Eds.), Reflection Seismology: A Global Perspective. Am. Geophys. Un. Geodynamics Series, vol. 13, pp. 301–311.

Petersen, T., 2000. Anzeichen für eine Magmakammer nördlich von Island, Diplomarbeit, Institut für Geowissenschaften, Abteilung Geophysik. Christian-Albrechts-Universität zu Kiel, Germany. http://www.geophysik.uni-kiel.de/wwwmar/TANJA/report.html.

Stern, R.J., Fouch, M.J., Klemperer, S.L., 2003. An overview of the Izu–Bonin–Mariana Subduction Factory. In: Eiler, J., Hirschmann, M. (Eds.), Inside the Subduction Factory. Am. Geophys. Un. Geophysical Monograph, vol. 138, pp. 175–222.

Taylor, B., Goodliffe, A.M., Moore, G.F., Oakley, A.J., Fryer, P., EW0202 Scientific Party, 2002. Multi-channel seismic images of the Mariana Trough: EW0202 initial results. EOS, Transactions - American Geophysical Union, vol. 83 (47), F1319 Fall Meet. Suppl.

Thinon, I., Matias, L., Rehault, J.P., Hirn, A., Fidalgo-Gonzalez, L., Avedik, F., 2003. Deep structure of the Armorican Basin (Bay of Biscay); a review of Norgasis seismic reflection and refraction data. Journal of the Geological Society of London 160, 99–116.

Yilmaz, O., 2001. Seismic Data Analysis: Processing, Inversion, and Interpretation of Seismic Data. Society of Exploration Geophysicists, Tulsa, Oklahoma. 2027 pp.